Cell Systems

Report

Genetic resonance in the p53 signaling network

Graphical abstract

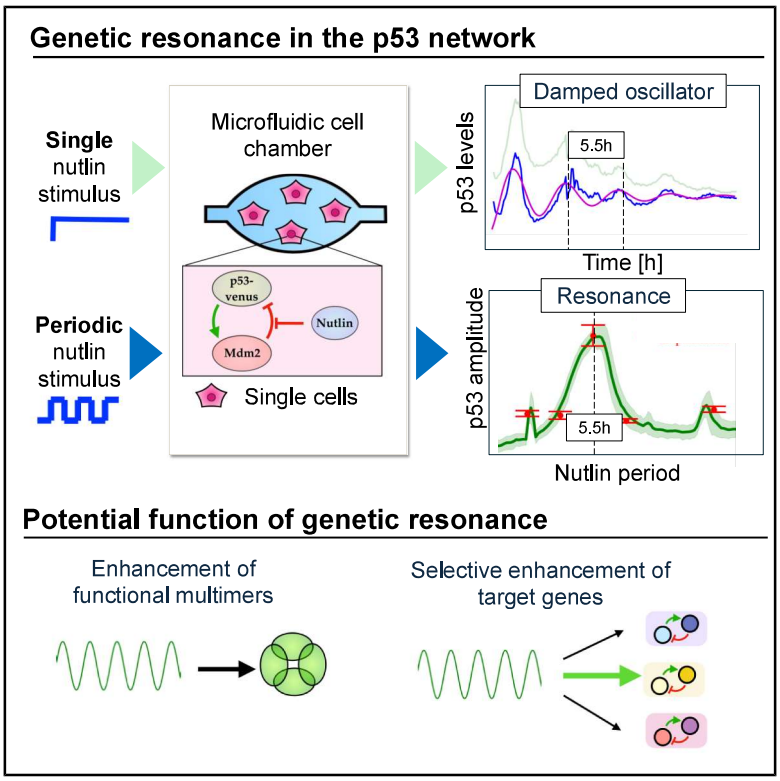

Authors

Mathias S. Heltberg, Alba Jimenez, Galit Lahav, Mogens H. Jensen

Correspondence

galit@hms.harvard.edu (G.L.), mhjensen@nbi.dk (M.H.J.)

In brief

Heltberg et al. showed that the tumor suppressor p53 behaves as a resonant system: a single stimulus induces damped oscillations, while periodic stimulation amplifies p53's natural rhythm. This reveals a striking parallel between a biological oscillator and physical oscillators and suggests resonance as a potential mechanism for selective gene activation.

Highlights

- A single chemical perturbation stabilizing the p53 protein leads to damped oscillations
- Periodic stabilization of p53 leads to oscillations with frequency-dependent amplitude
- Maximum amplitude, reflecting resonance, is observed at the natural p53 period
- Minor amplified peaks suggest nonlinear resonance

Heltberg et al., 2026, Cell Systems *17*, 101514
March 18, 2026
https://doi.org/10.1016/j.cels.2025.101514

CellPress

Cell Systems

CellPress

Report

Genetic resonance in the p53 signaling network

Mathias S. Heltberg,[1,3] Alba Jimenez,[2,3] Galit Lahav,[2,*] and Mogens H. Jensen[1,4,*]
[1]Niels Bohr Institute, University of Copenhagen, 2100 Copenhagen, Denmark
[2]Department of Systems Biology, Blavatnik Institute at Harvard Medical School, Boston, MA, USA
[3]These authors contributed equally
[4]Lead contact
*Correspondence: galit@hms.harvard.edu (G.L.), mhjensen@nbi.dk (M.H.J.)
https://doi.org/10.1016/j.cels.2025.101514

SUMMARY

Resonance allows systems to amplify their response to periodic stimuli and is well established in physics but not yet described in gene regulatory networks. Here, we asked whether resonance exists in the dynamics of p53, a tumor suppressor that oscillates after DNA damage to activate growth-inhibitory pathways. We developed a mathematical framework predicting that p53 exhibits damped oscillations after a single stimulus and frequency-dependent amplitudes under periodic stimulation, both hallmarks of resonance. Using live single-cell imaging, we confirmed these predictions: a single drug pulse that stabilizes p53 produced damped oscillations, while periodic pulses triggered frequency-dependent responses with maximal amplitudes at the natural p53 oscillation frequency as well as minor peaks. Finally, theoretical analysis suggested that resonance may enhance transcriptional responses and selectively activate downstream targets. Together, our results identify resonance as a regulatory principle in gene networks, potentially linking oscillations of transcription factors with selective gene activation through signal amplification.

INTRODUCTION

Resonance is a fundamental physical phenomenon, describing a system that shows a selective response to an external periodic signal, resulting in a maximal amplitude at a specific frequency. First described by Galileo Galilei and later solved mathematically by Leonard Euler,[1,2] resonance has marked a paradigm in physical and engineering research, with applications such as electrical resonance,[3,4] acoustic resonance,[5,6] nuclear magnetic resonance,[7] and many others. In the physical sciences, many phenomena are explained using the theory of resonance, from ocean tides[8] and climate changes of the Earth through stochastic resonance,[9] to emission and absorption of gamma radiation by atomic nuclei, known as the Mössbauer effect.[10] Consequently, Richard Feynman proposed that every issue of *Physical Review Letters* publishes at least one resonance curve.[11]

For a system to exhibit a resonant response, it first needs to be characterized as a damped oscillator.[11] A classic example of a damped oscillator is a spring. When triggered by an external stimulus, it undergoes damped oscillations with amplitudes that gradually decay due to energy loss from friction. At steady state, it no longer shows oscillations but still has a hidden characteristic frequency, which can become apparent following a new external stimulus. A periodic external signal stimulating a damped oscillator can result in frequency-dependent amplitudes, with a maximum amplitude obtained at a specific period—a hallmark of resonance (Figure 1A).

From a mathematical perspective, damped oscillations typically result from negative feedback loops (NFLs) (Figure 1B, top). NFLs are commonly found in biological networks[12,13] and are crucial for maintaining stability and homeostasis. The eigenvalues derived from the equations describing NFLs provide information about the system's characteristic frequencies,[14] which can be reflected in damped or undamped oscillations when the system is perturbed (Figure 1B, bottom). Indeed, many systems in living organisms exhibit rhythms and oscillations, including well-established circadian rhythms,[15–17] calcium oscillations,[18] pacemaker cells,[19] cell cycle,[20] and transcription factor (TF) responses such as the tumor suppressor protein p53 and the pro-inflammatory factor nuclear factor κB (NF-kB).[21–23]

Here, we focused on the oscillatory behavior of the tumor suppressor protein p53 as a model system for investigating resonance in biological systems. p53 is regulated by an NFL with Mdm2,[24] a transcriptional target of p53 and an E3 ubiquitin ligase promoting p53 degradation (Figure 1C).[25,26] In normal conditions, p53 levels remain low due to constant degradation by Mdm2. DNA damage disrupts the interaction between Mdm2 and p53, resulting in oscillations in p53 levels.[21,27,28] We first showed theoretically that resonance can appear in simulations of mathematical models describing the p53/Mdm2 NFLs. Nonlinear resonance effects led to small peaks at harmonic and subharmonic frequencies, occurring at integer and fractions of the resonant peak frequency, respectively. We then investigated the dynamic behavior of p53 in single cells and revealed that, in response to a single inhibition of Mdm2, p53 levels exhibit damped oscillations. Furthermore, in response to periodic inhibition of Mdm2, p53 exhibits sustained undamped oscillations with a frequency-dependent amplitude. Interestingly, the resonant

Please cite this article in press as: Heltberg et al., Genetic resonance in the p53 signaling network, Cell Systems (2025), https://doi.org/10.1016/j.cels.2025.101514

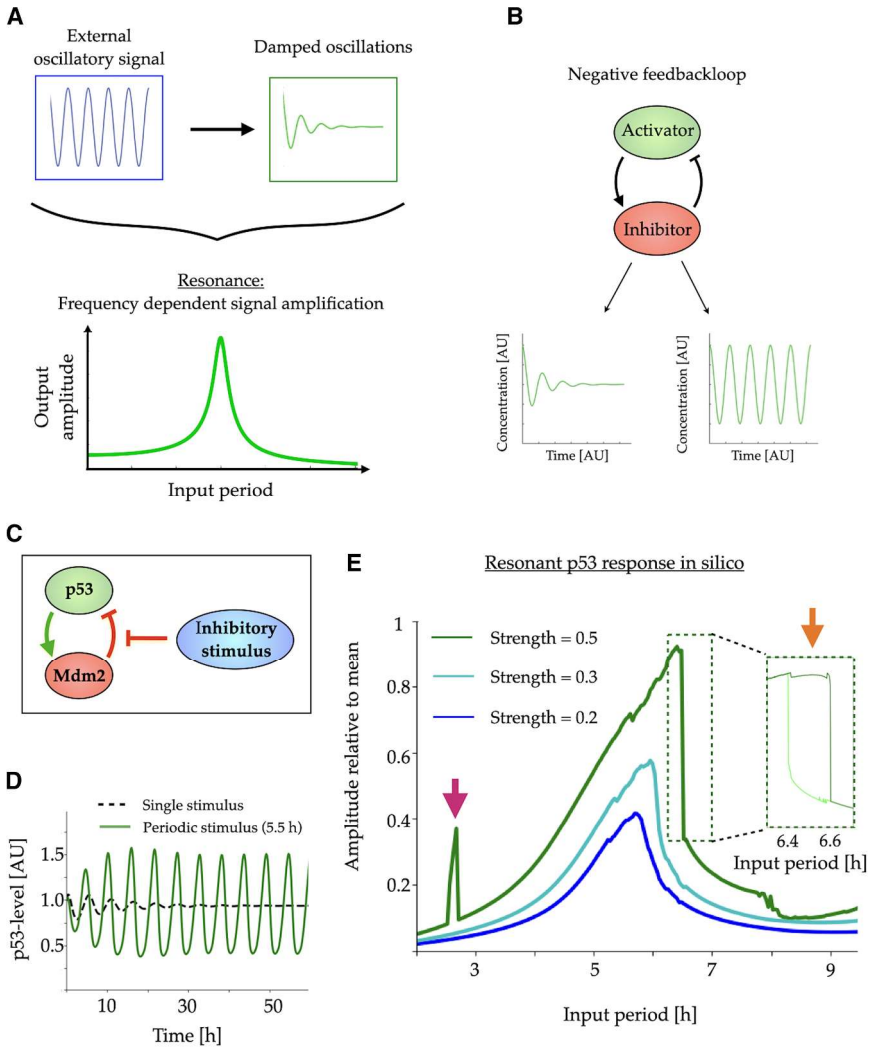

Figure 1. Resonance is theoretically predicted to appear in the p53 network

(A) An external oscillatory signal (input) simulating a damped oscillator can result in resonance with period-dependent amplitude (output).

(B) Negative feedback loops (NFLs) are common in gene regulatory networks and can give rise to damped oscillations or sustained undamped oscillations, depending on their feedback parameters.

(C) Schematic illustration of the p53/Mdm2 NFL. p53 activates the transcription of Mdm2, whereas Mdm2 marks p53 for degradation. Stimulation of the p53/Mdm2 feedback can be achieved by inhibition of their interactions.

(D) Simulation of p53 dynamics in response to a single stimulus (dotted black line) and to periodic external pulses (green line).

(E) p53 amplitude as a function of input period simulated for three input strengths. The magenta arrow highlights a nonlinear effect of peak at half internal period. The orange arrow indicates a small region of the nonlinear effect leading to hysteresis.

peak matched the natural frequency of p53 in response to DNA damage and strongly matched the theoretical simulations. We concluded the study by theoretically exploring possible functions for resonance and oscillatory TF, including amplification of transcriptional activity and selective gene expression.

RESULTS

Theory predicts the possibility of resonance in p53 dynamics

We hypothesized that p53, in its basal unperturbed conditions, may retain a hidden eigenfrequency and therefore show damped oscillations if perturbed. We first investigated this *in silico* by formulating a set of coupled differential equations describing the p53/Mdm2 NFL.[29] We modeled a scenario in which the main NFL was inhibited (Figure 1C). Simulation of this model (see STAR Methods) predicted that, in response to a single stimulus, p53 undergoes damped oscillations followed by homeostasis (Figure 1D, dotted black line). In response to periodic perturbations, the model predicted continuous oscillatory behavior of p53 (Figure 1D, green line).

To investigate whether resonance can exist in the p53 system, we mathematically simulated the p53 response to periodic stimulation with different frequencies. Our *in silico* analysis predicted that p53 exhibits a resonance curve with a peak (maximum amplitude) at an external frequency of around 5.5 h, which matches the natural frequency of p53 oscillations in response to DNA damage in human cells (Figure 1E, blue curve).[21,27,28] Enhancing the strength of the external stimulus led to an increase in the amplitude of p53 across different input strengths (Figure 1E). The strongest simulated input (0.5) resulted in a non-symmetric resonance curve (Figure 1E, green) with additional peaks around harmonic fractions of the characteristic frequency (Figure 1E, green curve, magenta arrow), typical for a nonlinear system.[30] In addition, we observed a small region in which the resonance curve was skewed to the right, suggesting bistability, in which both high-amplitude and low-amplitude solutions are present for the same frequency. This was also reflected by hysteresis, a phenomenon in which the path of the system's response differs between increasing and decreasing inputs (Figure 1E, green curve, orange arrow).[31,32] These mathematical results indicate that the p53/Mdm2 NFL can theoretically exhibit resonant behavior.

Experiments confirm damped oscillations of p53 following a single stimulus

To experimentally test the plausibility of resonance in p53 behavior, we first examined whether p53 acts as a damped oscillator following a single external stimulus, as predicted by the model (Figure 1D). Cells expressing a fluorescent p53 reporter[33] were subject to 1 μM nutlin, a compound that inhibits Mdm2 and

Please cite this article in press as: Heltberg et al., Genetic resonance in the p53 signaling network, Cell Systems (2025), https://doi.org/10.1016/j.cels.2025.101514

CellPress

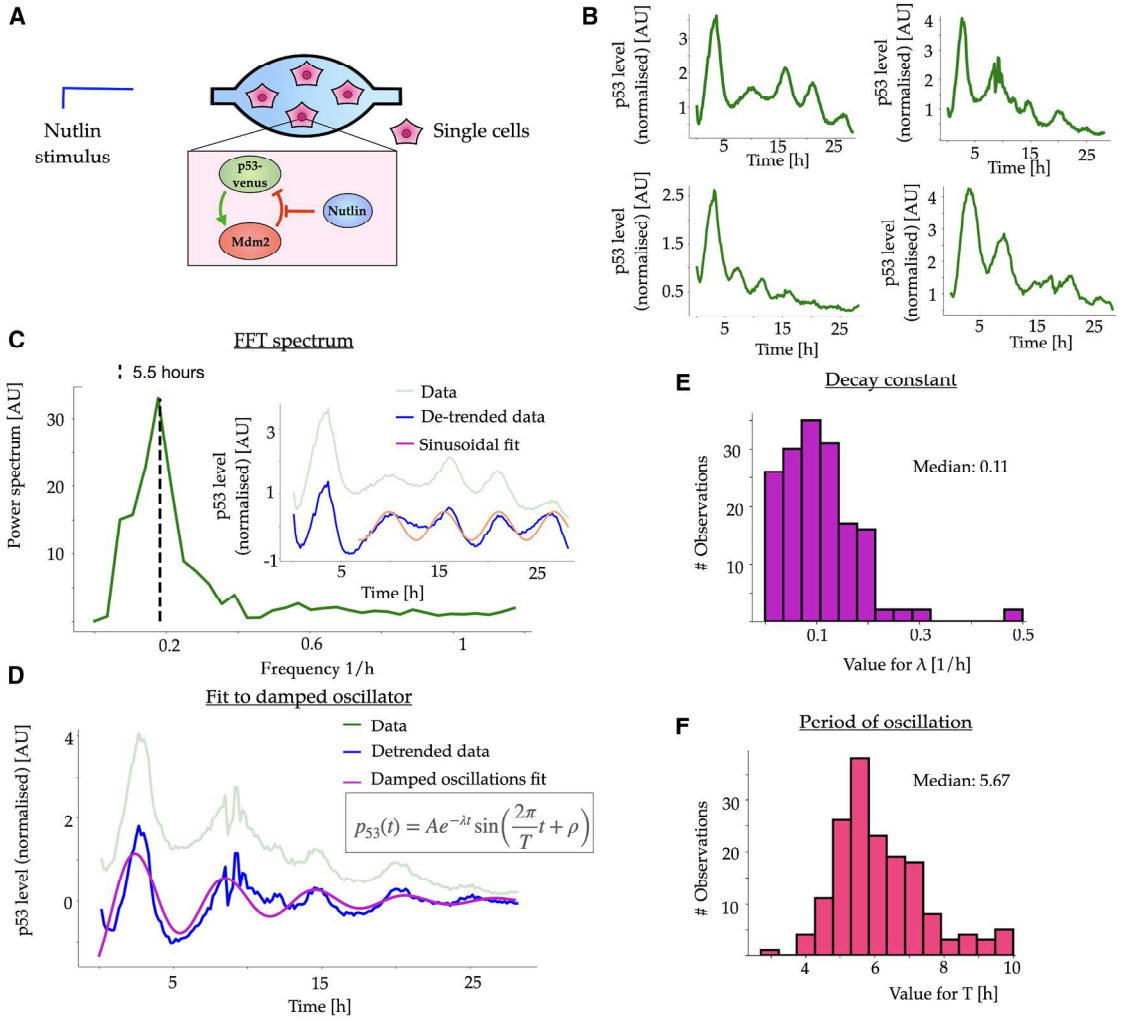

Figure 2. p53 shows damped oscillations in response to a single nutlin treatment

(A) Schematic illustration of the experimental setup and the Mdm2/p53 feedback. Levels of p53-YFP (yellow fluorescent protein) are measured in single cells stimulated with the small molecule nutlin, which disturbs the interaction between Mdm2 and p53.

(B) Four representative single-cell time series of p53 dynamics following a single treatment with 1 μM nutlin.

(C) Example of a fast Fourier transform (FFT) spectrum for a single-cell time series of p53 dynamics. (Inset) Detrended data (blue) and the sinusoidal function with frequency corresponding to the peak in the FFT signal (orange).

(D) Data (green), detrended data (blue), and exponential decaying fit with four free parameters (magenta).

(E and F) Distribution of the decay parameter (E) and the period (F) from fitting single-cell trajectories as in (D). n = 169 cells.

has previously been used to alter p53 dynamics (Figure 2A).[34,35] We then imaged cells for over 24 h and quantified the dynamics of p53 in individual cells. We found that a single treatment of nutlin led to one large p53 pulse followed by damped oscillations (Figure 2B). To analyze this behavior, we first computed the power spectrum of the dynamics following the initial p53 pulse and revealed an oscillatory signal with a frequency of approximately 5.5 h (Figure 2C), along with a strong fit between single-cell trajectories and the corresponding sinusoidal dynamics (Figure 2D, inset). We next used these fits to extract the eigenfrequencies and oscillation decay rates for trajectories obtained from single cells (Figure 2D). The distribution of the decay constants (γ) revealed a median of 0.11/h (Figure 2E), and the periods (T) showed a median of 5.67 h (Figure 2F). Taken together, these results reveal that following a single stimulation with nutlin, the p53/Mdm2 NFL acts as a damped oscillator with periods close to the ones observed following DNA damage.

Experiments confirm resonance in p53 dynamics in response to periodic stimuli

Based on the mathematical simulations (Figure 1E) and the observation that p53 shows damped oscillations in response to a single nutlin stimulus (Figure 2), we predicted that repeated periodic nutlin stimulation would trigger a series of p53 oscillations and that a nutlin input with a period of approximately 5.5 h would lead to maximal amplitudes of these oscillations. To test this, we developed a microfluidic device that controls the influx and efflux of media within a cellular culture environment (Figure 3A). This setup

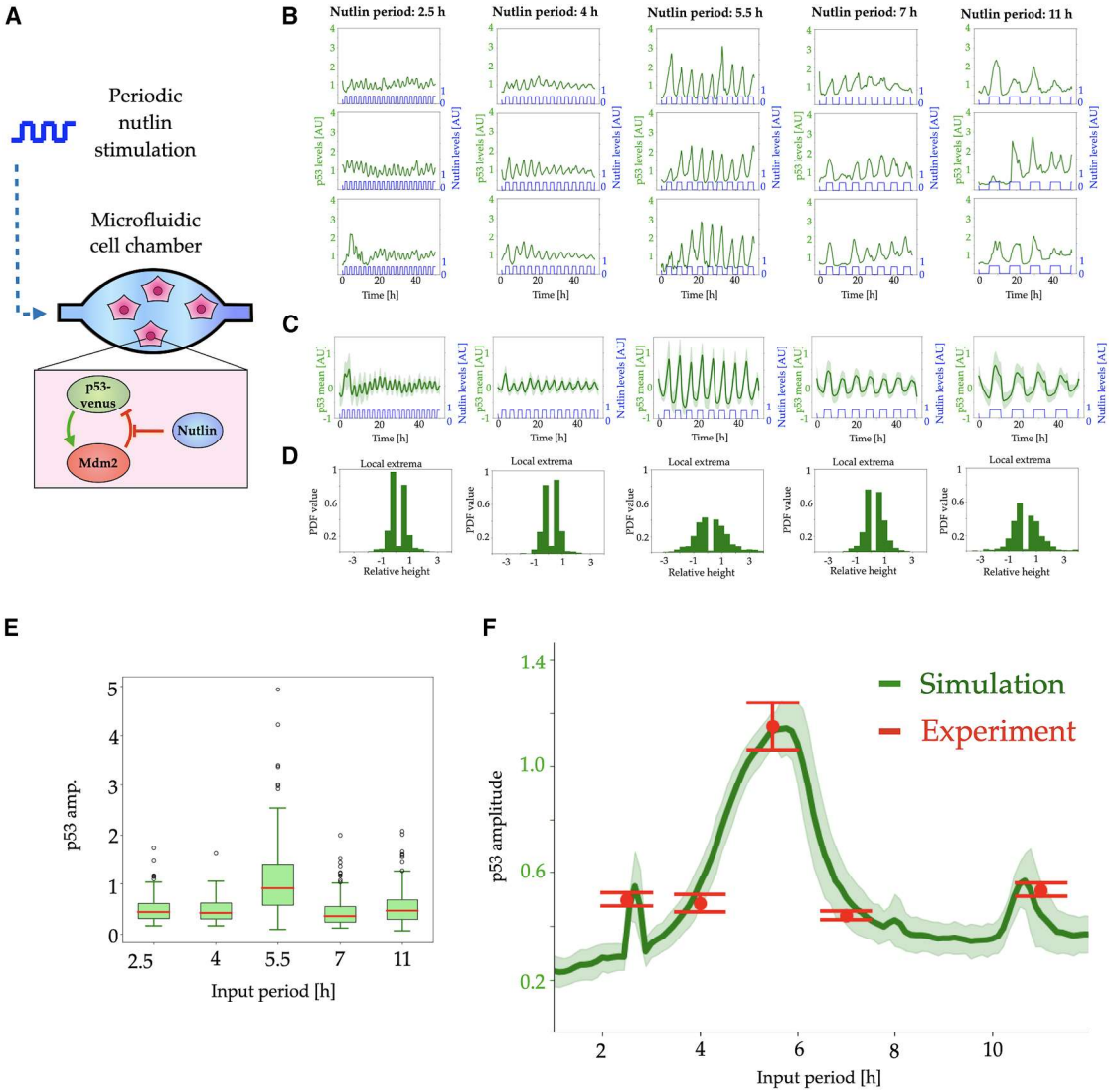

Figure 3. Resonance is experimentally detected in p53 dynamics

(A) Schematic illustration of the experimental setup and the Mdm2/p53 feedback. Levels of p53-YFP are measured in single cells treated with periodic nutlin stimulation using a microfluidic cell chamber.

(B) Representative examples of p53 traces from single cells (green) in response to five different nutlin periods (blue).

(C) Population mean (green dark line) and standard deviation of the mean (green shadows) in response to five different nutlin periods (blue).

(D) Distributions of p53 local extrema for the various nutlin periods across all cells.

(E) Boxplot showing all the amplitudes for each cell. Red lines indicate the median. n = 824 cells total.

(F) Mean and standard deviation of the mean of the experimentally measured p53 amplitude in response to different nutlin periods (red) compared with numerical simulations with 10% extrinsic noise in all the parameters. Green line, median; shaded region, standard deviation.

allows precise, periodic switching between drug-free media and media containing nutlin, providing controlled dosing conditions during imaging (see STAR Methods). We subjected cells to a range of periodic nutlin treatments and monitored p53 reporter levels in single cells for 50 h (Figure 3B). We found that p53 levels oscillated across all the examined nutlin periods, with oscillation periods that mimics the period of nutlin treatment. Notably, this behavior differs from entrainment, as it arises from an external periodic input perturbing a damped oscillator at steady state, whereas entrainment involves two sustained oscillators synchronizing to a common frequency.

We next set out to determine the relationship between nutlin period and p53 amplitude. As predicted by our model, p53 amplitude in response to nutlin administered with a 5.5-h period was the largest compared with slower or faster nutlin periods (Figure 3C). Note that at steady state, p53 shows spontaneous fluctuations,[36] and therefore its first peak amplitude can vary dramatically depending on its initial levels. Indeed, we found no correlation between the first p53 amplitude and the mean amplitude of subsequent pulses. We therefore analyzed p53 amplitude under each nutlin period by computationally identifying the local extrema in the p53 traces starting from the second

Please cite this article in press as: Heltberg et al., Genetic resonance in the p53 signaling network, Cell Systems (2025), https://doi.org/10.1016/j.cels.2025.101514

CellPress

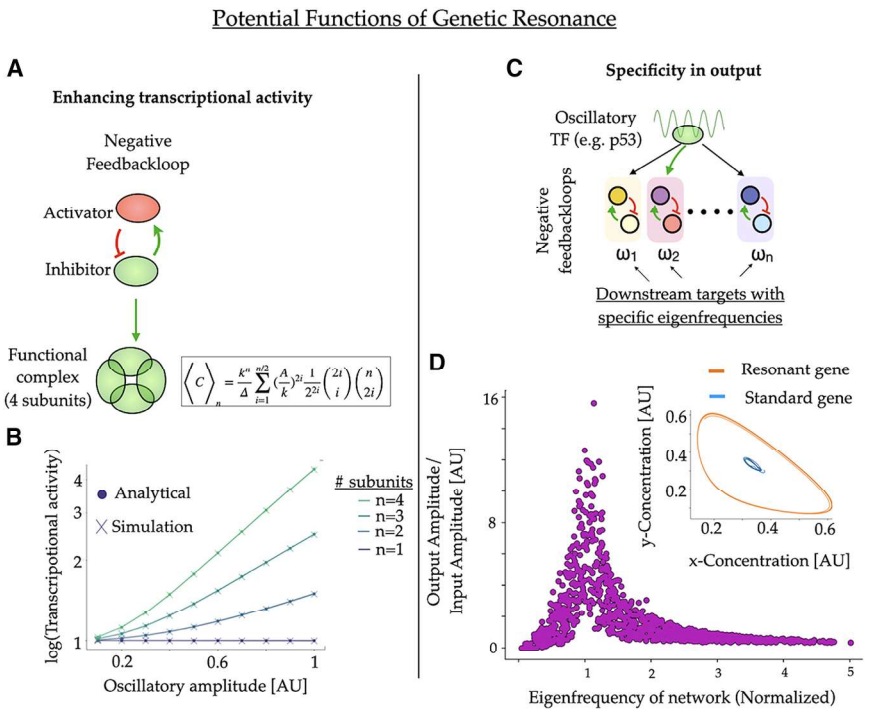

Figure 4. Potential function of genetic resonance

(A) Schematic illustration of a NFL and the formation of functional protein complexes required for the activation of downstream targets.

(B) Mean level of protein complexes as a function of an oscillatory amplitude for complexes with n subunits, shown for numerical simulations and analytical expressions. In the equation, A is the amplitude of oscillations, k is its mean value, and Δ is the degradation rate of the protein complex.

(C) Schematic illustration showing an oscillatory TF activating multiple downstream NFLs with various eigenfrequencies (ω_i).

(D) Amplitude of target genes (output) normalized to the amplitude of oscillatory TF (input), as a function of eigenfrequency for 1,000 random downstream NFLs. Eigenfrequencies were normalized to the TF oscillatory period. (Inset) Oscillating limit cycle of downstream targets involved in NFL for non-resonant genes (blue) and resonant genes (orange).

pulse (Figure 3D). We detected a resonance peak when we quantified the amplitudes across all cells (Figure 3E, bottom; Mann-Whitney U test, $p < 10^{-11}$). A similar pattern was found by deriving the mean amplitude for each nutlin period (Figure 3F, red points).

According to the classical theory of linear resonance, the amplitude-versus-frequency curve exhibits a single peak, with amplitudes decreasing to the left and right of the peak. Based on this, the null hypothesis is that the p53 amplitudes in response to periods of 11 and 2.5 h would be smaller than those at 4 and 7 h, respectively. Our experimental measurements revealed a departure from this expected pattern. The amplitudes for 11 and 2.5 h periods were slightly larger than the ones for 7 and 4 h, respectively (Mann-Whitney U test, $p = 0.003$ and $p = 0.37$) (Figures 3E and 3F). The appearance of minor sub- and super-harmonic peaks may result from nonlinearity of the p53 oscillator, although we cannot conclusively state that nonlinear resonance is the sole mechanism underlying this behavior.[30] Mathematical simulation of p53 responses to external periods ranging from 1–12 h closely matched the experimental results (Figure 3F), strengthening the possibility of nonlinear resonance within p53 dynamics and confirming that the p53/Mdm2 NFL reaches maximal response amplitudes at frequencies close to its natural oscillation period following DNA damage.

Potential functions of resonance in genetic networks

We next sought to theoretically explore the potential functional role of resonance in biology. It has previously been observed that an increase in the amplitudes of TF oscillations enhances the concentration of their downstream targets.[37–40] Since p53's transcriptional activity and its binding to DNA require the formation of tetramers (dimer of dimers), and many other TFs form homodimers (Figure 4A), we derived the average concentration of protein complexes with n components as a function of their oscillation amplitude (Figure 4B). We found that higher amplitudes enhance the formation of homodimers with larger n complexes, resulting in higher concentrations of the functional protein complexes (Figure 4B). Comparing this analytical result to simulations (Figure 4B; see STAR Methods) showed strong agreement. It should be noted that there is no enhancement in functionality for monomers—only higher-order complexes are enhanced by higher amplitudes. Thus, resonance in p53, resulting in maximum amplitude at its natural period, is predicted to enhance the concentration of its tetrameric complexes and therefore its transcriptional activity.

Since we have shown that resonance exists in the p53 network, we hypothesize that other NFLs with complex eigenvalues may also exhibit resonant responses. We therefore used p53 oscillatory behavior in response to DNA damage as the source of periodic stimulus and investigated its effect on hypothetical targets genes with distinct eigenfrequencies, ω_i (Figure 4C). We constructed a simple two-component NFL, activated by an oscillatory input of p53 and ran 1,000 simulations with random parameters. All simulations were constrained to be stable, with a fixed decay rate of 0.1/h, similar to p53 oscillations after DNA damage. The eigenfrequency of each NFL therefore was dependent on the random parameters and, for simplicity, was normalized to the period of the p53 oscillator. Our simulations revealed that only a fraction of target genes is strongly amplified by p53 oscillations after DNA damage (Figure 4D, inset orange), while many are minimally affected (Figure 4D, inset blue). Analysis of the amplitude of all downstream targets revealed a resonance curve, with the highest induction obtained at eigenfrequencies equal or close to those

Please cite this article in press as: Heltberg et al., Genetic resonance in the p53 signaling network, Cell Systems (2025), https://doi.org/10.1016/j.cels.2025.101514

of the p53 oscillator. This suggests that oscillations in a key TF, such as p53, may serve to selectively enhance targets whose NFL eigenfrequencies match the period of the upstream signal.

DISCUSSION

The phenomenon of resonance has been studied and applied in engineering and physics for centuries; however, it has yet to be seen in biological signaling. Here, we combined theoretical simulations with live single-cell imaging experiments to uncover resonance within the p53/Mdm2 NFL. We found that external periodic perturbation of p53 at steady state results in oscillations that match the external period and exhibit frequency-dependent amplitudes. In the classical theory of resonance, maximal amplitude is obtained under one specific frequency. However, NFLs involving nonlinear interactions may result in additional resonance peaks and hysteresis. Our model predicted both behaviors (Figure 1E). We were unable to experimentally detect hysteresis, most likely since it exists within a frequency window of only a few minutes. However, we were able to detect minor resonance peaks at half and double the optimal period (Figures 3E and 3F), suggesting a nonlinear resonance phenomenon. Further testing how the input strength (nutlin concentration) affects the height of the sub- and super-harmonic peaks will be required to validate and uncover the existence of nonlinearity in this system. Interestingly, the highest amplitude of p53 oscillations resulted from an external period similar to the p53 period in response to DNA damage in human cells (5.5 h). It was recently shown that the frequency of p53 oscillations in mice is faster (≈ 2.7 h) due to enhanced p53/Mdm2 feedback,[41] raising the question of whether a resonant peak in mouse cells exists at this shorter period.

It is important to discuss in what ways our work is distinct from other studies examining the effect of frequency-dependent responses. First, the term "frequency" can refer either to the total number of occurrences or to the number of periodic peaks of an oscillator per time. The influential work by Elowitz and coworkers[42] outlined how frequency, in terms of total numbers of bursts, can affect gene regulation. In our study, we refer specifically to the periodic frequency of an oscillator and its impact on the output amplitude, which can only be achieved by an oscillatory source. It is also critical not to confuse resonance with entrainment. Entrainment has been studied in various biological systems. For example, it was shown that external oscillations can adjust the oscillatory frequency of NF-κB.[37,43,44] In addition, the landmark paper by Zambrano et al.[45] demonstrated the ability of a biological oscillator to synchronize through phase and frequency entrainment. Even in the context of p53, we have recently discovered synchronization, entrainment, and the emergence of complex behaviors in response to an external periodic stimulus.[46] The distinction between these studies of entrainment and our work is crucial: entrainment modifies oscillation frequency through the effect of one oscillator on the other, whereas resonance enhances the amplitude of the output based on the input frequency by stimulating a damped oscillatory system at its homeostatic steady state. Our study therefore focuses on the effect on p53 under basal growth conditions when p53 levels are at low steady state and do not oscillate. This approach allows detecting signatures of resonance while avoiding the influence of other pathways that might affect the cellular state following DNA damage.

Experimentally, it has been shown that oscillations can be used to identify NFL structures based on characteristics of the response,[47] and that triggering NFL with an oscillatory signal can provide fundamental insight into their structure and specific dynamical features.[46] We suspect that resonance may exist in other oscillatory TFs that form NFLs, such as NF-κB.[45] Resonance and its theoretical functional role in stimulating specific downstream targets based on oscillatory frequency may explain the mechanism by which downstream targets of oscillating NF-κB are differentially stimulated at various frequencies.[37] For the p53 system, it has so far been challenging to vary its frequency. The experimental system presented here offers new approaches for varying p53 frequency and investigating the effect on tetramerization state (the functional units of p53) and choice of downstream programs, which will help determine whether resonance indeed enhances selective target genes, as proposed here by our theoretical model.

Taken together, our work revealed that the physical phenomenon of resonance can emerge in the genetic p53 network. We believe that this discovery will prompt the scientific community to investigate resonance in additional systems with NFLs. Should resonance be unveiled across additional genetic circuits, it would mark a great leap in our understanding of the function of oscillations in biology. It would be exciting if a fundamental physical principle such as resonance also proves to have functional relevance in the core networks of living organisms.

Limitations of the study

In this study, we show that the p53 peak in response to external perturbation with a period of 5.5 h is significantly larger than the amplitudes obtained at other periods. Since the amplitudes at 2.5 and 11 h are slightly larger than the amplitudes observed at 4 and 7 h, respectively, we suggest the existence of nonlinearity. Firmly confirming such a potential nonlinear nature will require additional measurement at higher resolution across external periods. We also acknowledge that, although we theoretically suggest a new mechanism for differentially stimulating downstream networks, we have not experimentally validated this mechanism. Performing such experiments will require global measurements of downstream target expression in response to various frequencies of p53. Finally, while we suggest that resonance could be fundamental for key TFs with hundreds of downstream targets, we have only shown the existence of resonance in the p53 network.

RESOURCE AVAILABILITY

Lead contact

Further information and requests for resources and reagents should be directed to and will be fulfilled by the lead contact, Mogens H. Jensen, mhjensen@nbi.dk.

Materials availability

All materials are either commercially available or can be available upon request.

Data and code availability

- All data and simulation code are publicly available at: https://github.com/MathiasHeltberg/GeneticResonanceInp53_CellSystems/tree/main/DataToUpload.

- Any additional information required to reproduce this work is available from the lead contact.

ACKNOWLEDGMENTS

We thank members of the Lahav and Jensen groups for their input and discussions. This work was funded by funding from the National Institutes of Health grant no. R35 GM139572 (G.L.) and the Ludwig Center at Harvard, United States (G.L.). Furthermore, this work was supported by the Novo Nordisk Foundation, Denmark (grant nos. NNF20OC0064978 and NNF24OC0089788, M.H.J., and grant no. NNF23OC0085907, M.S.H.); the Lundbeck Foundation, Denmark (grant no. R347-2020-2250, M.S.H.); and European Research Council, European Union (ERC grant no. 101221324, PHOSCIL, M.S.H.).

AUTHOR CONTRIBUTIONS

Planning and conceptualization, M.S.H., A.J., G.L., and M.H.J.; simulations and mathematical analysis, M.S.H.; experimental design, A.J. and G.L.; carrying out the experiments, A.J.; analysis of the experimental results, M.S.H. and A.J.; writing the manuscript, M.S.H., A.J., G.L., and M.H.J.; editing the manuscript, M.S.H., A.J., G.L., and M.H.J.

DECLARATION OF INTERESTS

The authors declare no conflicts of interest.

STAR★METHODS

Detailed methods are provided in the online version of this paper and include the following:

- KEY RESOURCES TABLE
- METHOD DETAILS
  - Experimental setup
  - Data analysis
  - Mathematical models

SUPPLEMENTAL INFORMATION

Supplemental information can be found online at .https://doi.org/10.1016/j.cels.2025.101514.

Received: July 3, 2024
Revised: March 14, 2025
Accepted: December 18, 2025

REFERENCES

1. Euler, L. (1750). De novo genere oscillationum. In Commentarii Academiae Scientiarum Petropolitanae (Petropoli), pp. 128–149.
2. Bistafa, S.R. (2022). Euler first theory of resonance. Arch. Hist. Exact Sci. *76*, 207–221. https://doi.org/10.1007/s00407-021-00280-5.
3. Hertz, H. (1887). Ueber sehr schnelle electrische Schwingungen. Ann. Phys. *267*, 421–448. https://doi.org/10.1002/andp.18872670707.
4. Thomson, W. (1853). LXV. On transient electric currents. Lond. Edinb. Dublin Philos. Mag. J. Sci. *5*, 393–405. https://doi.org/10.1080/14786445308647279.
5. Von Helmholtz, H. (2013). Die Lehre von den Tonempfindungen als physiologische Grundlage für die Theorie der Musik (Springer-Verlag). https://www.digitale-sammlungen.de/view/bsb10598685?page=5.
6. Rayleigh, J.S.B., and Baron, S. (1896). The Theory of Sound Vol. 2 (Macmillan).
7. Rabi, I.I., Zacharias, J.R., Millman, S., and Kusch, P. (1938). A new method of measuring nuclear magnetic moment. Phys. Rev. *53*, 318. https://doi.org/10.1103/PhysRev.53.318.
8. Godin, G. (1993). On tidal resonance. Contin. Shelf Res. *13*, 89–107. https://doi.org/10.1016/0278-4343(93)90037-X.
9. Benzi, R., Sutera, A., and Vulpiani, A. (1981). The mechanism of stochastic resonance. J. Phys., A: Math. Gen. *14*, L453–L457. https://doi.org/10.1088/0305-4470/14/11/006.
10. Mossbauer, R.L. (1958). Kernresonanzfluoreszenz von gammastrahlung in Ir191. Z. Physik *151*, 124–143. https://doi.org/10.1007/BF01344210.
11. Feynman, R.P., Leighton, R.B., Sands, M., and Hafner, E.M. (1965). The Feynman Lectures on Physics; Vol. I. Am. J. Phys. *33*, 750–752. https://doi.org/10.1119/1.1972241.
12. Yeger-Lotem, E., Sattath, S., Kashtan, N., Itzkovitz, S., Milo, R., Pinter, R.Y., Alon, U., and Margalit, H. (2004). Network motifs in integrated cellular networks of transcription–regulation and protein–protein interaction. Proc. Natl. Acad. Sci. USA *101*, 5934–5939. https://doi.org/10.1073/pnas.0306752101.
13. Kashtan, N., and Alon, U. (2005). Spontaneous evolution of modularity and network motifs. Proc. Natl. Acad. Sci. USA *102*, 13773–13778. https://doi.org/10.1073/pnas.0503610102.
14. Alon, U. (2006). An Introduction to Systems Biology: Design Principles of Biological Circuits (Chapman and Hall/CRC). https://doi.org/10.1201/9781420011432.
15. Zehring, W.A., Wheeler, D.A., Reddy, P., Konopka, R.J., Kyriacou, C.P., Rosbash, M., and Hall, J.C. (1984). P-element transformation with period locus DNA restores rhythmicity to mutant, arrhythmic Drosophila melanogaster. Cell *39*, 369–376. https://doi.org/10.1016/0092-8674(84)90015-1.
16. Hardin, P.E., Hall, J.C., and Rosbash, M. (1990). Feedback of the Drosophila period gene product on circadian cycling of its messenger RNA levels. Nature *343*, 536–540. https://doi.org/10.1038/343536a0.
17. Bargiello, T.A., Jackson, F.R., and Young, M.W. (1984). Restoration of circadian behavioural rhythms by gene transfer in Drosophila. Nature *312*, 752–754. https://doi.org/10.1038/312752a0.
18. Goldbeter, A. (2002). Computational approaches to cellular rhythms. Nature *420*, 238–245. https://doi.org/10.1038/nature01259.
19. O'Rourke, B., Ramza, B.M., and Marban, E. (1994). Oscillations of membrane current and excitability driven by metabolic oscillations in heart cells. Science *265*, 962–966. https://doi.org/10.1126/science.8052856.
20. Tsai, T.Y.-C., Choi, Y.S., Ma, W., Pomerening, J.R., Tang, C., and Ferrell, J.E., Jr. (2008). Robust, tunable biological oscillations from interlinked positive and negative feedback loops. Science *321*, 126–129. https://doi.org/10.1126/science.1156951.
21. Lahav, G., Rosenfeld, N., Sigal, A., Geva-Zatorsky, N., Levine, A.J., Elowitz, M.B., and Alon, U. (2004). Dynamics of the p53-Mdm2 feedback loop in individual cells. Nat. Genet. *36*, 147–150. https://doi.org/10.1038/ng1293.
22. Nelson, D.E., Ihekwaba, A.E., Elliott, M., Johnson, J.R., Gibney, C.A., Foreman, B.E., Nelson, G., See, V., Horton, C.A., Spiller, D.G., et al. (2004). Oscillations in NF-κB signaling control the dynamics of gene expression. Science *306*, 704–708. https://doi.org/10.1126/science.1099962.
23. Hoffmann, A., Levchenko, A., Scott, M.L., and Baltimore, D. (2002). The IκB-NF-κB signaling module: temporal control and selective gene activation. Science *298*, 1241–1245. https://doi.org/10.1126/science.1071914.
24. Wu, X., Bayle, J.H., Olson, D., and Levine, A.J. (1993). The p53-mdm-2 autoregulatory feedback loop. Genes Dev. *7*, 1126–1132. https://doi.org/10.1101/gad.7.7a.1126.
25. Haupt, Y., Maya, R., Kazaz, A., and Oren, M. (1997). Mdm2 promotes the rapid degradation of p53. Nature *387*, 296–299. https://doi.org/10.1038/387296a0.
26. Kubbutat, M.H., Jones, S.N., and Vousden, K.H. (1997). Regulation of p53 stability by Mdm2. Nature *387*, 299–303. https://doi.org/10.1038/387299a0.
27. Geva-Zatorsky, N., Rosenfeld, N., Itzkovitz, S., Milo, R., Sigal, A., Dekel, E., Yarnitzky, T., Liron, Y., Polak, P., Lahav, G., et al. (2006). Oscillations

and variability in the p53 system. Mol. Syst. Biol. *2*, 2006.0033. https://doi.org/10.1038/msb4100068.

28. Batchelor, E., Mock, C.S., Bhan, I., Loewer, A., and Lahav, G. (2008). Recurrent initiation: a mechanism for triggering p53 pulses in response to DNA damage. Mol. Cell *30*, 277–289. https://doi.org/10.1016/j.molcel.2008.03.016.
29. Mengel, B., Hunziker, A., Pedersen, L., Trusina, A., Jensen, M.H., and Krishna, S. (2010). Modeling oscillatory control in NF-κB, p53 and Wnt signaling. Curr. Opin. Genet. Dev. *20*, 656–664. https://doi.org/10.1016/j.gde.2010.08.008.
30. Kartashova, E. (2010). Nonlinear Resonance Analysis: Theory, Computation, Applications (Cambridge University Press). https://doi.org/10.1017/CBO9780511779046.
31. Jordan, D.W., and Smith, P. (2007). Nonlinear Ordinary Differential Equations: an Introduction for Scientists and Engineers (Oxford University Press). https://doi.org/10.1093/oso/9780199208241.001.0001.
32. Rand, R.H. (1994). Topics in Nonlinear Dynamics with Computer Algebra, vol. 1 (CRC Press).
33. Stewart-Ornstein, J., and Lahav, G. (2017). p53 dynamics in response to DNA damage vary across cell lines and are shaped by efficiency of DNA repair and activity of the kinase ATM. Sci. Signal. *10*, eaah6671. https://doi.org/10.1126/scisignal.aah6671.
34. Heltberg, M.S., Lucchetti, A., Hsieh, F.-S., Minh Nguyen, D.P.M., Chen, S.-H., and Jensen, M.H. (2022). Enhanced DNA repair through droplet formation and p53 oscillations. Cell *185*, 4394–4408.e10. https://doi.org/10.1016/j.cell.2022.10.004.
35. Purvis, J.E., Karhohs, K.W., Mock, C., Batchelor, E., Loewer, A., and Lahav, G. (2012). p53 dynamics control cell fate. Science *336*, 1440–1444. https://doi.org/10.1126/science.1218351.
36. Loewer, A., Batchelor, E., Gaglia, G., and Lahav, G. (2010). Basal dynamics of p53 reveal transcriptionally attenuated pulses in cycling cells. Cell *142*, 89–100. https://doi.org/10.1016/j.cell.2010.05.031.
37. Kellogg, R.A., and Tay, S. (2015). Noise facilitates transcriptional control under dynamic inputs. Cell *160*, 381–392. https://doi.org/10.1016/j.cell.2015.01.013.
38. Heltberg, M.S., Jiang, Y., Fan, Y., Zhang, Z., Nordentoft, M.S., Lin, W., Qian, L., Ouyang, Q., Jensen, M.H., and Wei, P. (2023). Coupled oscillator cooperativity as a control mechanism in chronobiology. Cell Syst. *14*, 382–391.e5. https://doi.org/10.1016/j.cels.2023.04.001.
39. Harton, M.D., Koh, W.S., Bunker, A.D., Singh, A., and Batchelor, E. (2019). p53 pulse modulation differentially regulates target gene promoters to regulate cell fate decisions. Mol. Syst. Biol. *15*, e8685. https://doi.org/10.15252/msb.20188685.
40. Heltberg, M.L., Krishna, S., and Jensen, M.H. (2019). On chaotic dynamics in transcription factors and the associated effects in differential gene regulation. Nat. Commun. *10*, 71. https://doi.org/10.1038/s41467-018-07932-1.
41. Stewart-Ornstein, J., Cheng, H.W.J., and Lahav, G. (2017). Conservation and divergence of p53 oscillation dynamics across species. Cell Syst. *5*, 410–417.e4. https://doi.org/10.1016/j.cels.2017.09.012.
42. Cai, L., Dalal, C.K., and Elowitz, M.B. (2008). Frequency-modulated nuclear localization bursts coordinate gene regulation. Nature *455*, 485–490. https://doi.org/10.1038/nature07292.
43. Heltberg, M., Kellogg, R.A., Krishna, S., Tay, S., and Jensen, M.H. (2016). Noise induces hopping between NF-κB entrainment modes. Cell Syst. *3*, 532–539.e3. https://doi.org/10.1016/j.cels.2016.11.014.
44. Mondragón-Palomino, O., Danino, T., Selimkhanov, J., Tsimring, L., and Hasty, J. (2011). Entrainment of a population of synthetic genetic oscillators. Science *333*, 1315–1319. https://doi.org/10.1126/science.1205369.
45. Zambrano, S., De Toma, I., Piffer, A., Bianchi, M.E., and Agresti, A. (2016). NF-κB oscillations translate into functionally related patterns of gene expression. eLife *5*, e09100. https://doi.org/10.7554/eLife.09100.
46. Jiménez, A., Lucchetti, A., Heltberg, M.S., Moretto, L., Sanchez, C., Jambhekar, A., Jensen, M.H., and Lahav, G. (2024). Entrainment and multi-stability of the p53 oscillator in human cells. Cell Syst. *15*, 956–968.e3. https://doi.org/10.1016/j.cels.2024.09.001.
47. Rahi, S.J., Larsch, J., Pecani, K., Katsov, A.Y., Mansouri, N., Tsaneva-Atanasova, K., Sontag, E.D., and Cross, F.R. (2017). Oscillatory stimuli differentiate adapting circuit topologies. Nat. Methods *14*, 1010–1016. https://doi.org/10.1038/nmeth.4408.
48. Reyes, J., Chen, J.-Y., Stewart-Ornstein, J., Karhohs, K.W., Mock, C.S., and Lahav, G. (2018). Fluctuations in p53 signaling allow escape from cell-cycle arrest. Mol. Cell *71*, 581–591.e5. https://doi.org/10.1016/j.molcel.2018.06.031.
49. Heltberg, M.L., Chen, S.H., Jiménez, A., Jambhekar, A., Jensen, M.H., and Lahav, G. (2019). Inferring leading interactions in the p53/Mdm2/Mdmx circuit through live-cell imaging and modeling. Cell Syst. *9*, 548–558.e5. https://doi.org/10.1016/j.cels.2019.10.010.

Please cite this article in press as: Heltberg et al., Genetic resonance in the p53 signaling network, Cell Systems (2025), https://doi.org/10.1016/j.cels.2025.101514

CellPress

STAR★METHODS

KEY RESOURCES TABLE

REAGENT or RESOURCE	SOURCE	IDENTIFIER
Deposited data		
Code for single cell analysis	This paper	Zenodo: 10.5281/zenodo.17297418
Experimental models: Cell lines		
MCF7p53YFP	Stewart-Ornstein and Lahav[33]	N/A
Chemicals, Peptides and Recombinant proteins		
Nutlin3A	Sigma	SML0580
Software and algorithms		
Custom Matlab Scriptsimage analysis	Stewart-Ornstein and Lahav[33]	N/A
Custom Python Scriptsentrainment analysis	This paper	Zenodo: 10.5281/zenodo.17297418

METHOD DETAILS

Experimental setup

Live-cell microscopy

MCF7 human cells expressing p53-YFP under the ubiquitin promoter, and a constitutively expressed nuclear marker (H2B-mCherry)[33] were grown in RPMI supplement with 10% FBS and antibiotics (100 mg/mL streptomycin, 250 ng/mL fungizone).

Two days before imaging, 20,000 cells were seeded onto 35mm poly-d-lysine-coated glass bottom plates (MatTek Corporation. 2 hrs before imaging, cell's media was replaced with transparent media (RPMI lacking riboflavin and phenol red, Invitrogen) and 5% FBS.

Imaging was conducted using a Nikon Eclipse TE-2000 inverted microscope with a 20× Plan Apo objective and a Hammamatsu Orca ER camera, equipped with environmental chamber controlling temperature, atmosphere (5% CO2) and humidity. Images were acquired every 10 minutes using the MetaMorph Software. Subsequent tracking and image analysis were executed using previously established protocols.[48] In brief, we used a semi-automated MATLAB-based method that tracks cells by identifying cell centroids using intensity and shape information of the constitutively expressed nuclear marker (H2B-mCherry),

Microfluidics device

The Arduino, an open-source electronics platform, was coupled with a set of hydraulic pumps to control periodic changes from drug-free media to media with nutlin, while cells were under the microscope. To dynamically control the exposure of cells to nutlin pulses during live imaging, a custom-built microfluidics system was designed. Cells were seeded onto 35mm poly-d-lysine-coated glass-bottom plates, which were covered with a plastic top drilled with two holes using a diamond bit and Dremel tool. Into these holes, two blunt-end, gauge 20 steel needles were inserted, each connected to 0.5 mm ID x 0.86 mm wall thickness silicone tubing (2.22 mm OD). One tube served for the fluid input, and the other as the output for fluid removal. Two peristaltic pumps (Langer Instruments, T60-S2 & WX10-14), operating at matched speeds, were used to maintain a stable 2 ml volume by ensuring equal rates of influx and efflux. The flow rate was adjusted to achieve gradual media exchanges that avoid disturbing cell adherence. Each media exchange lasted for 5 minutes. The influx tubing was connected to an Arduino-controlled valve, which uses a simple IF command to switch the input media between two bottles: one containing drug-free RPMI transparent media, and the other containing RPMI supplemented with nutlin. By adjusting the switching frequency, we controlled the timing of nutlin exposure.

Data analysis

We started by fitting a second-degree polynomial to the first pulse of p53 and calculated its height and position. We then applied Chauvenet's criterion to discard small fraction of non-responding cells or cells with diverging concentrations. Next, we fitted the dynamics after the first p53 pulse with a first-degree polynomial fit, and re-applied Chauvenet's criterion. With this method we ended up with a dataset of 169 cells out of the 222 that were imaged. This resulted in a dataset of trajectories whose dynamical features can be statistically examined.

To extract the frequency and decay constant of the p53 damped oscillator, we applied Scipy's Fast-Fourier Transform, which directly extracts the oscillations period. This period was then used as initial value for the final fit, which was performed using the Scipy optimize library based on least squares fit. Local peaks and valleys were defined as the highest or lowest values respectively, in the vicinity of +/-6 datapoints.

Please cite this article in press as: Heltberg et al., Genetic resonance in the p53 signaling network, Cell Systems (2025), https://doi.org/10.1016/j.cels.2025.101514

Mathematical models

Model of p53 dynamics

$$\frac{dp}{dt} = k_1 - \frac{k_2}{1+n} M \frac{p}{k_3 \frac{1}{1+n} + p} \quad \text{(Equation S1)}$$

$$\frac{dm}{dt} = k4p^2 - k_5 m$$

$$n(t) = \frac{A}{2}\left(1 + sgn\left(sin\left(\frac{2\pi}{T_{Ext}} t\right)\right)\right)$$

The p53-Mdm2 circuit was simulated using the differential equations below:

Here p, m, and M represent the concentrations of p53, Mdm2-mRNA, and Mdm2, respectively. In this model, p53 is produced at a fixed rate (k_1) and degraded following binding to Mdm2 via a saturated degradation process (k_2, k_3). The Mdm2-mRNA is produced proportionally to the square of the p53 level reflecting the dimeric action of p53 with a scaling production parameter (k_4) and is degraded through a first-order decay process (k_5). Finally, the protein Mdm2 is synthesized in proportion to the Mdm2-mRNA concentration with a constant rate (k_6) and is similarly subjected to first-order decay (k_7). Stimulation with nutlin (n), was introduced as a dimensionless variable that impacts the degradation of p53. This framework strives to minimize the number of parameters while adequately capturing the dynamics of the system. Parameter values were determined to recapitulate the previously described p53 low steady levels in normal growth conditions and oscillations with a frequency of approximately 5.5 hours in response to DNA damage.[21,49] For parameter values we used: k_1 = 3.0 μM h^{-1} k_2 = 4.5 h^{-1}, k_3 = 0.5 μM, k_4 = 0.3 μM^{-1} h^{-1}, k_5 = 1 h^{-1}, k_6 = 1 h^{-1} and k_7= 0.7 h^{-1}.

Simulation of downstream targets

We consider a biochemical negative feedback loop between species x and y that can be described by the following equations:

Tracking software available at: https://github.com/balvahal/p53CinemaManual

$$\dot{x} = -cx = ay = dx^2 \quad \text{(Equation S2)}$$

$$\dot{y} = A_1 \, sin(\omega t) + b - ay - dx^2 \quad \text{(Equation S3)}$$

By finding the fixed points and calculating the Jacobian we find the real part of the fixed point to be:

$$2\lambda_R = -c - a + 2d\frac{b}{c}\frac{bc^2}{ac^2 + b^2 d} - d\frac{b^2}{c^2} \quad \text{(Equation S4)}$$

Fixing \lambda_R = −0.1 we isolate the parameter a and define:

$$a = \frac{1}{2}\left(-\beta + \sqrt{\Delta}\right) \quad \text{(Equation S5)}$$

with

$$\beta = 2\lambda_R + c + 2c^2\frac{d}{c^2} \quad \text{(Equation S6)}$$

and

$$\Delta = \beta^2 - 4\left(2\lambda_R b^2 \frac{d}{c^2} - b^2\frac{d}{c} + d^2\frac{b^4}{c^4}\right) \quad \text{(Equation S7)}$$

Where parameters b,c, and d are chosen from random distributions with b=A_1·3·Rn, c=5·Rn and d=20·Rn; Rn being a uniformly distributed parameter between 0 and, and b > A_1 for the stimulation to be positive. The numbers we multiply the random number by (3, 5, and 20) are chosen to get a numerically stable simulation while still obtaining a spread in the eigenfrequency.

Derivation of protein complex concentration

The concentration of a protein complex, C, made of n components, is described by the differential equation:

$$\frac{dC}{dt} = (p(t))^n - \Delta C \text{ with } p(t) = k + A \sin(\omega t) \quad \text{(Equation S8)}$$

Please cite this article in press as: Heltberg et al., Genetic resonance in the p53 signaling network, Cell Systems (2025), https://doi.org/10.1016/j.cels.2025.101514

Here the first term on the right side represents the concentration of the components needed to make up C. We imagine this to be a protein part of a resonant network, but this derivation could also be applicable to genes stimulated by oscillatory transcription factors that work as complexes. Now this can be solved by:

$$\frac{dC}{dt} + \Delta C = k^n\left(1+\frac{A}{k}\sin(\omega t)\right)^n \quad \text{(Equation S9)}$$

$$\Longrightarrow \frac{dU}{dt} = k^n\left(1+\frac{A}{k}\sin(\omega t)\right)^n e^{\Delta t} \text{ with } U = Ce^{\Delta t} \quad \text{(Equation S10)}$$

Starting with n = 1 we get:

$$U(t) = k\int_0^1\left(1 + \frac{A}{k}\sin(\omega t')\right)e^{\Delta t'}dt' \quad \text{(Equation S11)}$$

$$= \frac{\boldsymbol{k}}{\Delta}\left(\boldsymbol{e^{\Delta t}} - 1\right) + \frac{\boldsymbol{A}}{\boldsymbol{k}}\frac{\boldsymbol{\omega} + (\Delta \boldsymbol{sin}(\boldsymbol{\omega t}) - \omega\cos(\omega t))e^{\Delta t}}{\boldsymbol{\Delta^2 + \omega^2}} \quad \text{(Equation S12)}$$

We see that terms with exp(-\Delta t) quickly dies off, and on average the terms involving sin and cos are zero. This means that the average level is simply:

$$(\langle C(t)\rangle)_{n=1} = \frac{k}{\Delta} \quad \text{(Equation S13)}$$

Expanding to larger n we get:

$$U(t) = k^n\int_0^t\left(1+\frac{A}{k}\sin(\omega t')\right)^n e^{\Delta t'}dt' \quad \text{(Equation S14)}$$

$$= \boldsymbol{k^n}\int_0^t\sum_{i=0}^{n}\binom{n}{k}\left(\frac{A}{k}\right)^i sin^i(\omega t')e^{\Delta t'}dt' \quad \text{(Equation S15)}$$

The expansion of sin ^n(ωt) can be written as:

$$sin^n\theta = \frac{2}{2^n}\sum_{k=0}^{\frac{n-1}{2}}(-1)^{\frac{n-1}{2}-k}\frac{n}{k}\sin((n-2k)\theta) \text{ if n is odd} \quad \text{(Equation S16)}$$

$$sin^n\theta = \frac{1}{2^n}\binom{n}{\frac{n}{2}} + \frac{2}{2^n}\sum_{k=0}^{\frac{n}{2}-1}(-1)^{\left(\frac{n}{2}-k\right)}\binom{n}{k}\cos((n-2k)\theta) \text{if n is even} \quad \text{(Equation S17)}$$

Since all terms except for the first term in the even expansion, are proportional to sin, we see that on average (and thereby in steady state) we get only a nonzero number for the even terms. This means we can write:

$$\langle C(t)\rangle_n = \frac{k^n}{\Delta}\sum_{i=1}^{n/2}\left(\frac{A}{k}\right)^{2i}\frac{1}{2^{2i}}\binom{2i}{i}\binom{n}{2i} \textit{if n is even} \quad \text{(Equation S18)}$$

$$\langle C(t)\rangle_n = \frac{k^n}{\Delta}\sum_{i=1}^{(n-1)/2}\left(\frac{A}{k}\right)^{2i}\frac{1}{2^{2i}}\binom{2i}{i}\binom{n}{2n} \textit{if n is odd} \quad \text{(Equation S19)}$$

This gives an exact connection between the average level of a protein complex as a function of the amplitude of oscillations in the subunits. Note that if TFs as p53 work as tetramers, we expect that the efficiency of downstream gene stimulation is enhanced following the same functional dependence.